

**Analysis of the mechanism which periodontopathic bacteria
induce vascular endothelial cell apoptosis**

(歯周病原性細菌が血管内皮細胞アポトーシスを誘導する
メカニズムの解析)

Nihon University Graduate School of Dentistry at Matsudo

Masaaki Hirasawa

(Director: Prof. Tomoko Ochiai)

日本大学大学院 松戸歯学研究科 歯学専攻

平澤 正晃

(指導： 落合智子教授)

Contents

1. Preface	3
2. Abstract	4
3. Introduction	6
4. Materials and Methods	10
4.1 Bacterial strain and culture methods	10
4.2 Cell line and reagents	10
4.3 Cell viability assay and cell proliferation assay	11
4.4 Measurement of cell death	11
4.5 Caspase assay	13
4.6 Measurement of intracellular ROS	14
4.7 Determination of endothelial nitric oxide production	14
4.8 Real-time quantitative RT-PCR	15
4.9 Antibodies and western blot analysis	16
4.10 siRNA knockdown	17
4.11 Acridine orange staining	17
4.12 Measurements of oxidative stress	18
4.13 Statistical analysis	18
5. Results	19
5.1 <i>P. gingivalis</i> 381 inhibits cell proliferation and induces cell death through apoptosis	19
5.2 ER stress is involved in <i>P. gingivalis</i> 381-induced apoptosis	20

5.3 <i>P. gingivalis</i> 381 contributes to ER stress-induced autophagy	21
5.4 <i>Aa</i> induces HUVEC apoptosis in HUVEC/monocyte co-culture system	22
5.5 <i>Aa</i> induces ROS production in monocytes	23
5.6 Upregulation of NADPH oxidase expression	23
5.7 H ₂ O ₂ induces HUVEC apoptosis	23
6. Discussion	25
7. Conclusion	31
8. References	32
9. Figures	40

1. Preface

This article is constructed with a main reference paper “*Porphyromonas gingivalis* induces apoptosis and autophagy via ER stress in human umbilical vein endothelial cells” in *Mediators of Inflammation*, and a reference paper “*Aggregatibacter actinomycetemcomitans* sensitized monocytes induce endothelial cell apoptosis” in *International Journal of Oral-Medical Science*.

2. Abstract

It has been reported that periodontitis is associated with an increased risk of atherosclerosis. Periodontal disease-related bacteria *Porphyromonas gingivalis* and *Aggregatibacter actinomycetemcomitans (Aa)* have been detected in atheromatous plaques and shown to accelerate the development of atherosclerosis in ApoE deficient spontaneously hyperlipidemic mice. Accumulating evidence suggests that endothelial dysfunction is an early marker for atherosclerosis. To determine how periodontal infections contribute to endothelial dysfunction, the effect of *P. gingivalis* and *Aa* on human umbilical vein endothelial cells (HUVEC) was examined. *P. gingivalis* significantly suppressed the viability of HUVEC and induced DNA fragmentation and annexin-V staining, and increased caspase-3, -8, and -9 activity. *P. gingivalis* also increased the expression of GADD153 and GRP78, and caspase-12 activity. Further, *P. gingivalis* induced autophagy, as evidenced by increased LC3-II and Beclin-1 levels. The suppression of *P. gingivalis*-induced autophagy by silencing of LC3 with siRNA significantly increased *P. gingivalis*-induced apoptosis. Endoplasmic reticulum (ER) stress inhibitor, salubrinal, suppressed apoptosis and autophagy by inhibiting *P. gingivalis*-induced DNA fragmentation, and LC3-II expression. These data suggest that *P. gingivalis* infection induces ER stress-mediated apoptosis followed by autophagic response that protects HUVEC from

P. gingivalis -mediated apoptosis, potentially amplifying proatherogenic mechanisms in the perturbed vasculature.

In the second part of the study, we examined the ability of the major periodontal pathogen, *Aa*-sensitized monocytes to modulate properties of HUVEC by assessment of reactive oxygen species (ROS) production and apoptosis. Cell proliferation and apoptosis was measured by BrdU cell proliferation ELISA kit, cell death detection ELISA and caspase activities. Detection of intracellular ROS generation was evaluated fluorometrically using H2DCF-DA. Quantitative reverse transcription polymerase chain reaction was performed using primers specific for p22phox and p47phox. iNOS, p22phox and p47phox in cell lysates were detected by Western blot analysis with the respective specific antibodies. *Aa* did not affect the viability of HUVEC but induced apoptosis in HUVEC cocultured with monocytes. *Aa* significantly induced ROS and NO productions in monocytes. Furthermore, *Aa* increased gene and protein expressions of p22phox, p47phox and iNOS. Also, H₂O₂ induced growth inhibition, apoptosis and caspase 3/7 activities in HUVEC. These results suggest that apoptosis in HUVEC could be induced by *Aa* -sensitized monocytes via ROS-dependent pathway, potentially amplifying proatherogenic mechanism in the perturbed vasculature.

3. Introduction

Periodontal disease is highly prevalent, affecting up to 90% of the global population [1]. *Porphyromonas gingivalis*, a major periodontal pathogen, was recently implicated in the pathogenesis of atherosclerosis [2]. *P. gingivalis* can directly access the systemic circulation and the endothelium in patients with periodontitis, as transient bacteremias are common [3]. Indeed, *P. gingivalis* has been detected in human atherosclerotic plaques [4] [5], and it can both invade endothelial cells (EC) and persist therein [6]. Further, *P. gingivalis* elicits a proatherogenic response in EC in the form of increased leukocyte adhesion with concomitant up-regulation of adhesion molecules and proinflammatory cytokines and chemokines [7] [8]. Interestingly, these effects require the invasion of EC by viable bacteria [8].

EC are key cellular components of blood vessels that function as a selectively permeable barrier between blood and tissue. It is believed that atherogenic risk factors induce apoptosis in EC, leading to the denudation or dysfunction of the intact endothelial monolayer, with subsequent atherosclerotic lesion formation as a result of lipid accumulation, monocyte adhesion, and inflammatory reactions [9] [10]. Endothelial cell apoptosis has several potential deleterious effects, including plaque erosion and thrombosis [11]. Recent studies have demonstrated increased endoplasmic reticulum (ER) stress protein expression in the vascular cells of atherosclerotic lesions, and regulation of the protein in the endothelium by

several atherosclerotic stressors [12].

Autophagy is a cellular defense mechanism involving degradation and recycling of cytoplasmic components. Autophagy can protect cells from apoptosis; thus, it is said to sit at the crossroad between cell death and survival. However, excessive autophagy can destroy essential cellular components and cause to cell death [13]. Accumulating evidence has also suggested that ER stress is linked to autophagy [14]. In the present study, the capacity of whole viable *P. gingivalis* to induce cell death via apoptosis, ER stress and autophagy in human umbilical vein endothelial cells (HUVEC) was examined.

Another potential pathway through which periodontitis may contribute to atherogenesis is through induction of oxidative stress [15]. Extensive production of reactive oxygen species (ROS) has been implicated in atherosclerosis by inducing the chronic activation of the vascular endothelium and components of the immune system. Vascular endothelial ROS released from nicotinamide adenine dinucleotide phosphate (NADPH) oxidase may play critical roles in ROS generation [16]. In humans, higher expression of NADPH oxidase subunit proteins is associated with increased superoxide ($O_2^{\cdot-}$) production and severity of atherosclerosis. NADPH oxidase-deficient *Apoe*^{-/-} mice had significantly less atherosclerosis compared with *Apoe*^{-/-} mice [17]. Further studies clearly demonstrated that superoxide production from both monocytes/macrophages and vascular cells plays a

critical role in atherogenesis [18]. Monocyte recruitment from the blood stream into the vessel wall is crucial for atherosclerosis lesion formation and progression. After endothelial dysfunction induced by factors including LDL, hypertension, or diabetes, monocytes attach to the endothelium and migrate into the subendothelial space where they take up lipid, become foam cells and cause early lesion development [19]. Monocytes induce lipid peroxidation via the generation of ROS. These modified lipids can induce the expression of adhesion molecules and mediators of inflammation in macrophages and vascular wall cells [20]. Monocyte-derived ROS impair endothelial function and accelerate the progression of atherosclerotic lesion by promoting lipid oxidation, the expression of proinflammatory genes, and endothelial cell apoptosis [21]. Therefore, detailed understanding of the regulation and signal transduction of ROS production in monocytes is important.

Endothelial cells are key cellular components of blood vessels, functioning as selectively permeable barriers between blood and tissues. It is believed that risk factors induce endothelial cell apoptosis, leading to the denudation or dysfunction of the intact endothelial monolayer, which causes lipid accumulation, monocyte adhesion, and inflammatory reactions that initiate atherosclerotic lesions [9] [10]. Although information on risk factor-induced atherosclerosis has been accumulating, the underlying mechanism remains unclear. The aim of this work was to study the induction of ROS and NO in

Aggregatibacter actinomycetemcomitans (Aa)-sensitized monocytes followed by apoptosis in HUVEC exposed to *Aa*-sensitized monocytes.

4. Materials and methods

4.1. Bacterial strains and culture methods

P. gingivalis strain 381 and KDP136 (gingipain-null mutant) were cultured on anaerobic blood agar plates (Becton Dickinson Co., Sunnyvale, CA) in a model 1024 anaerobic system (Forma Scientific, Marietta, OH) under 10% H₂, 80% N₂ and 10% CO₂ for 3 - 5 days. The cells were then inoculated into brain heart infusion broth (Difco Laboratories, Detroit, MI) supplemented with 5 µg/ml hemin and 0.4 µg/ml menadione and cultured to an OD₆₆₀ of 0.8 (10⁹ cfu/mL). *Aa* HK1651 (ATCC 700685) was grown in Todd-Hewitt broth (BBL, Cockeysville, MD, USA) supplemented with 1% yeast extract (Difco Laboratories, Detroit, MI, USA) at 37°C in 5% CO₂ for 3 days until it reached an OD_{540nm} of 0.55, corresponding to 10⁹ CFU/mL. The cells were then harvested by centrifugation at 8,000 × *g* for 20 min at 4°C and diluted in phosphate-buffered saline (PBS).

4.2. Cell line and reagents

HUVEC (provided by Lonza-Takara, Tokyo, Japan) were cultured at 37°C in a humidified atmosphere with 5% CO₂ in endothelial cell culture medium (EGM-2 BulletKit; Lonza-Takara). Acute monocytic leukemia (THP-1) cells were purchased from the Health Science Research Resources Bank and cultured in RPMI1640 containing 10% fetal bovine serum, 10 mM HEPES, 100 µU/ mL penicillin, and 100 µg/mL streptomycin (Invitrogen, Tokyo,

Japan). All experiments were performed on cells at passages 4-8 at approximately 80% confluence. N-acetyl-L-cystein (NAC) was purchased from Wako. iNOS inhibitor 1400W was purchased from Sigma (St Louis, MO, USA).

4.3. Cell viability assay and cell proliferation assay

Cell viability was determined using a Cell Counting Kit-8 (CCK-8; Wako, Osaka, Japan). Briefly, cells (1.0×10^4 /well) were cultured in 100 μ L of endothelial cell culture medium in a 96-well plate and stimulated with *P. gingivalis* at the indicated multiplicity of infection (MOI). After 19 h, 10 μ L of CCK-8 solution was added, and the cells were incubated at 37°C for 2 h, followed by measurement of A450 using a spectrophotometer. In the second experiments, cell proliferation was determined using a BrdU cell proliferation ELISA kit (Calbiochem, Darmstadt, Germany). Briefly, cells (2.0×10^4 /well) were cultured in 200 μ L of endothelial cell culture medium in a 48-well plate and stimulated with *Aa* at the indicated multiplicity of infection (MOI) or H₂O₂. After 16 h, 40 μ L of BrdU solution was added, and the cells were incubated at 37°C for 2 h, followed by measurement of A450 using a spectrophotometer.

4.4. Measurement of cell death

Cellular apoptosis was quantified by DNA fragmentation using the Cell

Death Detection ELISA^{PLUS} kit (Roche Diagnostics, Mannheim, Germany). Briefly, HUVEC (5×10^5 /dish) were cultured with *P. gingivalis* 381 and KDP136 strains at the indicated MOI. After 7, 16, and 24 h, the cells were lysed in 200 μ L of lysis buffer, and 20 μ L of the supernatant was reacted with 80 μ L of anti-DNA immunocomplex conjugated with peroxidase, which interacts with streptavidin-coated wells, in a microtiter plate for 2 h. At the end of the incubation, 100 μ L of substrate was added, and color development was quantified as a wavelength of 405 nm. The results were calculated as the ratio of the absorbance of the *P. gingivalis*-treated cells to the absorbance of the non-treated control cells. For the apoptosis inhibition assays, cells were preincubated for 1 h with caspase-12 inhibitor Z-VAD-FMK (MBL, Nagoya, Japan) or ER stress inhibitor, salubrinal (50 μ M) (Sigma-Aldrich, St. Louis, MO, USA) before stimulation with the bacteria. Apoptosis of the *P. gingivalis*-treated HUVEC was assessed by annexin V-EnzoGold and 7-amino-actinomycin D (7-AAD) staining (Enzo Life Sciences Inc., Farmingdale, NY) and flow cytometric analysis using a FACSCalibur Flow Cytometer (Becton Dickinson, Franklin Lakes, NJ). In the second experiment, cellular apoptosis was also quantified by DNA fragmentation using the Cell Death Detection ELISA^{PLUS} kit (Roche, Mannheim, Germany). HUVEC (2.0×10^4 /well) or HUVEC co-cultured with THP-1 cells (2.0×10^4 /well) (HUVEC/THP-1) were incubated with *Aa* at an MOI of 10, 100, or 1000 for 16 h. HUVEC was indirectly cocultured with THP-1 cells using 4 μ m

pore size cell culture inserts within a 24-well plate (BD falcon, Franklin Lakes, NJ). HUVEC was also co-cultured for 16 h with tenths volume of culture supernatant of THP-1 cells sensitized with *Aa* for 16 h. The cells were lysed in 200 μ L of lysis buffer, and 20 μ L of the supernatant was reacted with 80 μ L of anti-DNA immunocomplex conjugated with peroxidase, which interacts with streptavidin-coated wells, in a microtiter plate for 2 h. At the end of the incubation, 100 μ L of substrate was added, and color development was quantified as a wavelength of 405 nm. For the apoptosis inhibition assays, THP-1 cells were preincubated for 1 h with the anti-oxidant NAC or inducible nitric-oxide synthase (iNOS) inhibitor 1400W before sensitization with *Aa*. Caspase 3/7 activity was measured using a Caspase-Glo 3/7 assay kit (Promega, Madison, USA).

4.5. Caspase assay

After incubation (5×10^5 cells/dish) for 16 h with *P. gingivalis* 381, the cells were harvested, and the caspase-1, -3, -8, -9 and -12 activities were measured using a caspase fluorometric protease assay kit (MBL). The amount of 7-amino-4-trifluoromethylcoumarine (AFC) released was measured using an ARVO Multilabel/Luminescence Counter with excitation and emission at 400 and 505 nm, respectively.

4.6. Measurement of intracellular ROS

Detection of intracellular ROS generation was evaluated fluorometrically using 2',7'-dichlorodihydrofluorescein diacetate (H2DCF-DA) [22]. THP-1 cells (5×10^5 cells/well in 24-well plates) were treated with *Aa*, followed by the addition of 50 μ L H2DCF-DA. After 30 min of incubation at 37°C, the cells were washed twice with PBS to remove any extracellular dye. The formation of the fluorescence spectrometer at excitation and emission wavelengths of 485 and 530 nm, respectively. DCFDA is deacetylated and reacts quantitatively with intracellular radicals such as H₂O₂ to produce a fluorescent product, dichlorofluorescein, which is retained within the cell and thus provides an index of cell cytosolic oxidation.

4.7. Determination of endothelial nitric oxide production

THP-1 cells (5×10^5 cells/well in 24-well plates) were treated with *Aa*, and production of NO by THP-1 cells was measured as its stable oxidation product; nitrite, using Bioxytech nitric oxide assay kit (OxisResearch; Portland, USA). Briefly, 50 μ L of the culture medium was diluted with 35 μ L assay buffer and mixed with 10 μ L nitrate reductase and 10 μ L NADH. Following 30 minutes of incubation to convert nitrate to nitrite, total nitrite was measured at 540 nm absorbance by reaction with Griess reagents

(sulfanilamide and naphthalene-ethylenediamine dihydrochloride).

4.8. Real-time quantitative RT-PCR

Quantitative RT-PCR was performed using primers specific for C/EBP homologous protein (CHOP)/ Growth arrest and DNA damage 153 (GADD153) (GGCAGCTGAGTCATTGCC and GCAGATTCACCATTCGGTCA), Glucose-regulated protein-78 (GRP78) (CCTAGCTGTGTCAGAATCTCCATCC and GTTTCAATGTCACCATCCAAGATCC), Beclin-1 (CCAGATGCGTTATGCCAGAC and CATTCCATTCCACGGGAACAC), Microtubule-associated protein 1 light chain 3B (MAP1LC3B) (ACGCATTTGCCATCACAGTTG and GGGACCTTCAGCAGTTTACAGTCAG), and β -actin (CATCCGTAAAGACCTCTATGCCAAC and ATGGAGCCACCGATCCACA). The thermal cycling profile was as follows: 95°C for 10 s followed by 40 cycles of 95°C for 5 s and 60°C for 30 s, with a final dissociation at 95°C for 5 s, 60°C for 30 s, and 95°C for 15 s. The starting amount of RNA was quantified using a standard curve; fold changes in the expression of CHOP/GADD153, GRP78, Beclin-1, and LC3B relative to β -actin were determined in triplicate.

In the second experiment, total RNA was isolated from *Aa*-treated THP-1 cells using an RNeasy kit (Qiagen, Hilden, Germany) according to the manufacturer's procedures. cDNA was synthesized using a PrimeScript RT

Reagent Kit (Perfect Real Time; Takara Bio). Real-time quantitative RT-PCR was performed using the Thermal Cycler Dice Real Time System TP800 and SYBR Premix Ex Taq II (Perfect Real Time; Takara Bio) according to the manufacturer's instructions. Primers specific for p22phox (forward, GCGCTTACCCAGTGGTACT; reverse, CTCCAGCAGGCACACAAACA), p47phox (forward, GGACACCTTCATCCGTCACATC; reverse, CAGGTCCTGCCATTTACCA), and GAPDH (forward, GCACCGTCAAGGCTGAGAAC; reverse, TGGTGAAGACGCCAGTGGA) were designed and produced by Takara Bio.

4.9. Antibodies and western blot analysis

Rabbit antibodies against GADD153, GRP78, Beclin-1, and β -actin were purchased from Santa Cruz Biotechnology, Inc. (Santa Cruz, CA), while those against LC-3 were purchased from MBL. Secondary Horseradish peroxidase (HRP)-conjugated goat anti-rabbit and goat anti-mouse antibodies were obtained from Amersham Pharmacia Biotech (Piscataway, NJ). In the second experiments, rabbit antibodies against iNOS, p22phox and p47phox were purchased from Santa Cruz Biotechnology Inc. (Santa Cruz, CA). Secondary HRP-conjugated goat anti-rabbit antibody was obtained from Amersham Pharmacia Biotech (Piscataway, NJ). Cells were lysed in a buffer containing 10 mM Tris-HCl, 150 mM NaCl, 1% Nonidet P-40, 1 mM Ethylenediaminetetraacetic acid (EDTA), 1 mM Ethylen glycol

tetraacetic acid (EGTA), 0.1 mM phenylmethylsulfonyl fluoride, 8 $\mu\text{g/ml}$ aprotinin, and 2 $\mu\text{g/ml}$ leupeptin (pH 7.4). For immunoblotting, proteins resolved by 12.5% sodium dodecyl sulfate-polyacrylamide gel (SDS-PAGE) were transferred to polyvinylidene fluoride membranes (Millipore, Bedford, MA), which were then exposed to primary and then secondary antibodies. Chemiluminescence detection was performed with an ECLTM Western Blotting Detection Kit (Amersham). The signal intensities of the corresponding bands were measured by a Light Capture equipped with CS Analyzer software (ATTO, Osaka, Japan).

4.10. siRNA knockdown

Knockdown of endogenous LC3 with siRNA was carried out using Lipofectamine RNAiMAX (Invitrogen) according to the manufacturer's instructions. Briefly, HUVEC grown to 50-80% confluence in a 6-well plate were transfected with either LC3B siRNA (sc-43391, Santa Cruz Biotechnology) or control siRNA (sc-37007, Santa Cruz Biotechnology). The final concentration of respective siRNA was 50 nM for each transfection, and the experiments were carried out 24 h after transfection.

4.11. Acridine orange staining

Cells were treated with *P. gingivalis* 381 at an MOI 1:10² for 8 h and stained with 1 mg/mL acridine orange at room temperature for 20 min. Then

cells were washed with PBS and visualized by fluorescence microscopy.

4.12. Measurements of oxidative stress

To directly monitor real time reactive oxygen/nitrogen species (ROS/RNS) a kit including an oxidative stress detection reagent (ENZO Life Sciences, Farmingdale, NY, USA) was used. THP-1 cells were infected with *Aa* at an MOI of 100 for 30 min and analyzed under fluorescence microscope.

4.13. Statistical analysis

All data are presented as means \pm SEM. Multiple-group comparisons were made by one-way analysis of variance, followed by *post hoc* intergroup comparison by the Bonferroni-Dunn test. A *p*-value < 0.05 was considered statistically significant.

5. Results

5.1.P. gingivalis 381 inhibits cell viability and induces cell death through apoptosis.

P. gingivalis 381 significantly diminished the viability of HUVEC at higher MOI (Fig. 1A). Next, we investigated whether the suppression of cell proliferation observed in HUVEC treated with *P. gingivalis* 381 was dependent on apoptosis. Incubation with *P. gingivalis* 381 strongly induced apoptosis in the HUVEC in a dose- and time-dependent manner (Fig. 1B). Higher apoptosis rates were observed at MOI of $1:5 \times 10^2$ after 16 h and $1:10^2$ and $1:5 \times 10^2$ after 24 h compared to the non-treated control group. In contrast, KDP 136 strain did not cause DNA fragmentation in any MOI and 24 h culture. In addition, we confirmed the possible apoptotic effect of *P. gingivalis* 381 by Annexin V and 7-AAD staining and flow cytometric analysis (Fig.1C). The early apoptotic cells represented by the lower right quadrant (7-AAD negative and Annexin V positive) and the non-viable necrotic and late-state apoptotic cells represented by the upper right quadrant (positive for Annexin V binding and 7-AAD uptake). After 21 h treatment with *P. gingivalis* 381 at an MOI of $1:10^2$, the number of early-stage apoptotic cells was significantly increased by up to $47.8 \pm 2.0 \%$ ($p < 0.01$). These results indicate that the decrease in viable cells induced by *P. gingivalis* 381 treatment is due to apoptosis. Apoptotic cell death typically occurs via the stimulation of caspase activity [23]. Caspase-8 and -9 appear

to be activated in the death receptor- and mitochondrial-dependent apoptotic pathways, respectively, and caspase-3, which is common to both pathways, induces DNA fragmentation. Pyroptosis, which is uniquely dependent on caspase-1, has been described in monocytes, macrophages, and dendritic cells infected with a range of microbial pathogens such as *Salmonella*, *Francisella*, and *Legionella* [24]. Therefore, we assessed the activity of caspase-1, -3, -8, and -9. *P. gingivalis* 381 enhanced caspase-3, -8, and -9 activity, suggesting involvement of the mitochondria-mediated intrinsic pathway and death receptor-induced extrinsic pathway (Fig. 1D). On the other hand, caspase-1 activity was not enhanced by *P. gingivalis* 381 within the range of the MOI investigated (data not shown). Therefore, cell death induced by *P. gingivalis* 381 was unrelated to pyroptosis.

5.2. ER stress is involved in P. gingivalis 381-induced apoptosis

To determine whether ER-mediated events contribute to *P. gingivalis* 381-induced apoptosis, we examined the levels of several substances reported to participate in ER-induced apoptosis and the unfolded protein response (UPR). Real-time PCR and Western blot analysis demonstrated that the ER stress-induced proteins or genes GADD153 and GRP78 were up-regulated by treatment with *P. gingivalis* 381 (Fig. 2A, B) although there was not so drastic but still significant difference in GRP78 mRNA level. A significant increase in caspase-12 activity at 21 h after the addition of *P.*

gingivalis 381 was also observed at MOI of 1:10 and 1: 10² (Fig. 2C).

Furthermore, DNA fragmentation induced by *P. gingivalis* 381 infection was significantly suppressed by pre-treatment with salubrinal and a caspase-12 inhibitor (Fig. 2D). *P. gingivalis* 381-induced caspase-3 and -12 activities were also completely abrogated by pre-treatment with salubrinal (Fig. 2E). These data suggest that the ER stress response functions prior to *P. gingivalis* 381-mediated apoptosis.

5.3. P. gingivalis 381 contributes to ER stress-induced autophagy

Autophagy is essential for the removal of damaged organelles and long-lived cytosolic macromolecules to maintain energy homeostasis, and hence cell survival, under starvation conditions. When excessive, however, autophagy results in autophagic cell death. To examine the connection between *P. gingivalis* 381 infection and the stimulation of autophagy, we examined the expression of Atg6 (Beclin-1) and the co-localization of LC3-II (both are autophagosome markers). Real-time PCR and Western blot analysis demonstrated that LC3-II and Beclin-1 were up-regulated by treatment with *P. gingivalis* 381 (Fig. 3A, B). In order to examine if autophagic signaling contributes to the protection against cell death, autophagy (a ratio of LC3-II/LC3-I) was suppressed by siRNA specific for LC3 (Fig. 3C). *P. gingivalis* 381 significantly increased apoptosis in autophagy-deficient HUVEC. These results suggest that autophagy induced

by *P. gingivalis* 381 protects HUVEC from apoptosis caused by the same bacteria.

Autophagy is also characterized by acidic vesicular organelle (AVO) formation, which can be assayed by acridine orange staining [25]. AVOs accumulated in the cytoplasm of HUVEC exposed to *P. gingivalis* 381 (Fig. 3D); however, this was inhibited by the addition of salubrinal (Fig. 3D). Furthermore, salubrinal suppressed *P. gingivalis* 381-induced LC3-II expression (Fig. 3E). These data suggest that the ER stress response functions prior to autophagy induced by *P. gingivalis* 381 infection.

5.4. Aa induces HUVEC apoptosis in HUVEC/monocyte co-culture system

We examined the effects of *Aa* on the proliferative activity of HUVEC by the BrdU ELISA after 16 h of incubation. At any MOI, the addition of *Aa* had little effect on HUVEC proliferation (Fig. 4A). On the other hand, *Aa* induced apoptosis in HUVEC in the presence of THP-1 cells (Fig. 4B). Higher apoptosis rates were observed at MOI of 100 and 1000 after 16 h compared to the non-treated control group. Next, we examined the effect of culture supernatant from THP-1 cells sensitized with *Aa*. THP-1 culture supernatant sensitized with *Aa* also induced apoptosis in HUVEC (Fig. 5A). In particular, significant apoptosis was observed when THP-1 was sensitized with MOI of 100 and 1000. On the other hand, apoptosis of HUVEC by *Aa*-sensitized THP-1 culture supernatant was significantly suppressed by

the addition of antioxidant (NAC) and iNOS inhibitor (1400 W)(Fig. 5B). These results suggest that active oxygen species contained in the culture supernatant of THP-1 sensitized with *Aa* may induce HUVEC apoptosis.

5.5. Aa induces ROS production in monocytes

Since apoptosis of HUVEC by *Aa*-sensitized THP-1 supernatant was suppressed by antioxidant (NAC) and iNOS inhibitor (1400W), we next investigated the production of ROS and NO from THP-1 by *Aa* -treatment. We found that in THP-1-producing ROS and NO, the amounts gradually increased in a concentration-dependent manner of *Aa* (Fig. 6A and 6B). In particular, production of ROS and NO at MOI: 100 was significantly higher than MOI: 10. As shown in Fig. 7, *Aa* significantly enhanced the generation of reactive species such as NO (Fig. 7A) and ROS (Fig. 7B).

5.6. Upregulation of NADPH oxidase expression

Real-time RT-PCR analysis showed that *Aa* increased gene expression levels of p22phox and p47phox in THP-1 cells (Fig. 8A and 8B). Sensitization of *Aa* to THP-1 cells was also induced protein expressions of iNOS, p47phox, and p22phox compared to non-treated THP-1 cells (Fig. 9).

5.7. H₂O₂ induces HUVEC apoptosis

We next examined the effects of hydrogen peroxide (H₂O₂), a reactive oxygen

species (ROS), on viability, apoptosis and caspase 3/7 activities in HUVEC (Fig. 10). Cell viability was significantly suppressed by high concentration (500-1000 μM) of H_2O_2 treatment. Cell death was significantly enhanced with medium to high concentration (250-1000 μM) of H_2O_2 treatment. Although caspase 3/7 activity was significantly enhanced by the medium concentration (250 μM) of H_2O_2 treatment, the activity sharply decreased with high concentration (500 to 1000 μM) of H_2O_2 treatment. These results raise the possibility that necrosis occurred at high concentrations of H_2O_2 treatment.

6. Discussion

In the first study, we found that HUVEC challenge with high doses of *P. gingivalis* 381 for 21h significantly exhibited suppression of viability. And it was found that this decrease in viability is cell death caused by endothelial apoptosis as evidenced by DNA fragmentation, Annexin-V staining, and caspase activity (Fig. 1A-D). Furthermore, since the challenge with KDP136 did not induce DNA fragmentation, it was suggested that the apoptosis - inducing factor in *P. gingivalis* 381 may be caused by gingipain (Fig. 1B). Caspase-3, -8 and -9 were significantly activated by intermediate-high doses of *P. gingivalis* 381 infection, suggesting that multiple signaling pathways were involved. Therefore, activation of these caspases may contribute to endothelial dysfunction. Pyroptosis is a more recently recognized form of regulated cell death with morphological and biochemical properties distinct from necrosis and apoptosis [24]. However, the death of the HUVEC in this study was unrelated to pyroptosis since caspase-1 activity was not changed at any *P. gingivalis* 381 dose examined (data not shown).

In this study, *P. gingivalis* 381 induced the expression of a number of ER stress markers, including GADD153, GRP78 and caspase-12, indicating that *P. gingivalis* 381 induces ER stress. The mRNA and protein levels of GADD153 and GRP78 were increased in MOI concentration-dependently except for the mRNA level of GADD153, but the Caspase-12 activity was

maximized at MOI (10) and decreased at MOI (10²). Because gingipain of *P. gingivalis* can cleave caspase-3 [26], cleavage of caspase-12 may be occurring at high concentration of MOI. Furthermore, since addition of either an ER stress inhibitor (salubrinal) or an anti-caspase-12 reagent significantly decreased *P. gingivalis* 381-induced apoptosis in HUVEC, ER stress may occur upstream rather than downstream of apoptosis in cells exposed to high doses of *P. gingivalis* 381. Therefore, the activation of ER stress markers such as GADD153, GRP78, and caspase-12 will likely to happen at an early stage compared with the factors related to apoptosis. Induction of the mammalian UPR involves, in part, enhanced transcription of genes encoding ER chaperones, including BiP/GRP78, which serves to correct protein misfolding. The UPR, which serves to restore cellular homeostasis, induces the transcription of genes encoding antiapoptotic and proapoptotic proteins. Thus, severe or prolonged ER stress may induce apoptosis. Again, our data suggest that *P. gingivalis* 381 induces apoptosis after ER stress. ER stress has been demonstrated at all stages of atherosclerotic lesion development in ApoE knockout mice, and it is evident in human atherosclerotic lesions [12] [27] [28]. However, the relationship between *P. gingivalis* 381 infection and ER stress is yet to be determined. Our preliminary data indicated that the infection with a higher *P. gingivalis* 381 MOI induced reactive oxygen species (ROS) in HUVEC (data not shown). It is known that ROS induces the ER stress [29] [30]. Further, it was also found that Lipopolysaccharide (LPS)

could activate the ER stress [31]. Therefore, ROS release in HUVEC and LPS by infection with *P. gingivalis* might induce the ER stress to HUVEC. Indeed, the expression levels of UPR-related genes were significantly higher in periodontitis compared with gingivitis lesions [32].

Accumulating evidence suggests that the ER plays an essential role not only in apoptosis but also in the regulation of autophagy [14] [33]. However, whether ER stress-mediated autophagy contributes to cell survival or cell death remains unclear. Here, we found that *P. gingivalis* 381-induced ER stress enhanced autophagy. The process of autophagosome formation depends on several autophagy proteins [34]. By translational modification of LC3, LC3-II (16 kDa) localizes exclusively to autophagosomal membranes and has been used as an autophagy marker [35]. We demonstrated that *P. gingivalis* 381 induced the expression of autophagy markers (e.g., Beclin-1, LC3-II and AVOs), and that LC3-II and AVOs expressions were inhibited by salubrinal. In addition, since specific suppression of LC3 by siRNA effectively downregulated LC3-II/LC3-I ratio and significantly increased the apoptosis in HUVEC upon stimulation with *P. gingivalis* 381, the autophagy may protect HUVEC from *P. gingivalis* 381-induced apoptosis. Most likely, autophagy under basal conditions plays an important role in cellular housekeeping, whereas induced autophagy may function as a death pathway, as suggested by our results.

In the second experiment, we previously demonstrated that *Aa* induced

endothelial apoptosis and atherosclerosis in spontaneously hyperlipidemic mice [36]. Therefore, this experiment was carried out considering that HUVEC apoptosis could be induced also in *Aa* infection as well as *P. gingivalis* infection. Contrary to expectation, *Aa* infection alone had no effect on the proliferation of HUVEC. Furthermore, *Aa* infection alone had no effect on HUVEC survival or apoptosis (data not shown). However, although co-culture of *Aa* and HUVEC had no effect on proliferation and apoptosis, co-existence of THP-1 resulted in a significant increase in apoptosis in HUVEC in proportion to MOI of *Aa*. On the other hand, since the enhancement of these apoptosis was significantly suppressed by the antioxidant NAC and the nitric oxide synthase inhibitor 1400W, it was thought that HUVEC apoptosis might be induced by the active oxygen and active nitrogen contained in the culture supernatant of *Aa*-stimulated THP-1 cells. Indeed, *Aa* produced ROS and NO from THP-1 cells in a MOI dependent manner.

NADPH oxidase, an oxidoreductase, is the mechanism of superoxide generation in living organisms which is currently receiving the most attention. This enzyme present on the cell membrane or membrane of the endoplasmic reticulum membrane oxidizes NADPH and generates superoxide. NADPH oxidase receives electrons from cytoplasmic NADPH and produces superoxide by one electron reduction of oxygen molecule [37]. Four kinds of isoforms of NADPH oxidase in the heart, NOX 1, NOX 2, NOX

4 and NOX 5 are known [38] [39]. NADPH oxidase is composed of cell membrane subunits NOX and p22phox and cytoplasmic subunits p67phox, p47phox and Noxal (NOX activator) [39]. Of these, NOX 4 is a type of constitutive enzyme, and it is characterized by being always activated. Recently, the activation of NOX4 is thought to be involved in the generation of hydrogen peroxide [39]. In NOX 1 and NOX 2 which is similar to the type present in granulocytes, the cytoplasmic subunits rac-GTPase, p47phox and p67phox migrate to the membrane, form a complex with NOX and p22phox of the cell membrane subunit, and express enzyme activity [39].

In this study, increased expression of p22phox and p47phox genes, which are subunits of NADPH oxidase, was observed by the adding *Aa* viable bacteria to THP-1 in the range of MOI: 10-10². Furthermore, *Aa* enhanced expression of iNOS, p22phox and p47phox proteins in THP-1 cells. Therefore, the production of ROS and NO in *Aa* sensitized THP-1 cells and the accompanying increase in NADPH expression suggest that *Aa* plays a central role in oxidative stress. Furthermore, it is known that ROS induces LDL oxidation and ER stress [29] [30]. Therefore, the release of ROS in HUVEC in the presence of *Aa*-sensitized THP-1 may induce ER stress on HUVEC. Indeed, the expression level of UPR-related genes was significantly higher in periodontitis than in gingivitis lesions [32].

There are various kinds of ROS in the living body, among them O₂⁻, H₂O₂ and hydroxyl radical (OH) are important [40]. Each of these reactive oxygen

species has different reactivity and half life, and each has its own characteristic. Hydrogen peroxide is produced not only by metabolic processes of superoxide but also by enzymatic reactions in vivo. H_2O_2 has weak toxicity, but its half-life is long, so once it is produced, it has a characteristic of staying relatively long, and when converted to OH, it causes cell damage. Therefore, given the half-life, ROS produced in the THP-1 culture supernatant may have existed in the form of H_2O_2 . Alternatively, it may have induced endothelial cell apoptosis in the form of exosomes containing NADPH oxidase [41].

Significant apoptosis of luminal endothelial cells has been reported in advanced human atherosclerotic plaques [42], a finding that is compatible with the onset role of endothelial apoptosis in plaque erosion. Our findings suggest that HUVEC apoptosis mediated by ROS [43] and NO [44] which were produced by monocytes sensitized with *Aa* may be partly involved in the development of atherosclerotic lesions by *Aa*.

7. Conclusion

In summary, the first part of data highlight the important relationships of ER stress and autophagy with apoptosis in HUVEC during *P. gingivalis* 381 exposure. The data also provide putative mechanisms for *P. gingivalis* 381-induced endothelial dysfunction, as well as suggesting potential strategies for the prevention of *P. gingivalis* 381-induced endothelial impairment.

In the second part of study, the data suggest that oxidative stress such as ROS and NO produced by *Aa*-sensitized monocytes may induce apoptosis in HUVEC. NADPH oxidase such as p22phox and p47phox, and iNOS were involved in the induction mechanisms of these oxidative stress. Therefore, this data also suggests to provide antioxidants as a potential strategy for the prevention of *Aa*-induced endothelial dysfunction.

8. References

1. Pihlstrom BL, Michalowicz BS, Johnson NW. Periodontal diseases. *Lancet*, 366:1809-1820, 2005.
2. Gibson FC, 3rd, Yumoto H, Takahashi Y, Chou HH, Genco CA: Innate immune signaling and *Porphyromonas gingivalis*-accelerated atherosclerosis. *J Dent Res*, 85:106-121, 2006.
3. Kinane DF, Riggio MP, Walker KF, MacKenzie D, Shearer B: Bacteraemia following periodontal procedures. *J Clin Periodontol*, 32:708-713, 2005.
4. Haraszthy VI, Zambon JJ, Trevisan M, Zeid M, Genco RJ: Identification of periodontal pathogens in atheromatous plaques. *J Periodontol*, 71:1554-1560, 2000.
5. Kozarov EV, Dorn BR, Shelburne CE, Dunn WA, Jr., Progulske-Fox A: Human atherosclerotic plaque contains viable invasive *Actinobacillus actinomycetemcomitans* and *Porphyromonas gingivalis*. *Arterioscler Thromb Vasc Biol*, 25:e17-18, 2005.
6. Dorn BR, Dunn WA, Jr., Progulske-Fox A: *Porphyromonas gingivalis* traffics to autophagosomes in human coronary artery endothelial cells. *Infect Immun*, 69:5698-5708, 2001.
7. Roth GA, Moser B, Huang SJ, Brandt JS, Huang Y, Papapanou PN, Schmidt AM, Lalla E: Infection with a periodontal pathogen induces

- procoagulant effects in human aortic endothelial cells. *J Thromb Haemost*, 4:2256-2261, 2006.
8. Roth GA, Moser B, Roth-Walter F, Giacona MB, Harja E, Papapanou PN, Schmidt AM, Lalla E: Infection with a periodontal pathogen increases mononuclear cell adhesion to human aortic endothelial cells. *Atherosclerosis*, 190:271-281, 2007.
 9. Xu Q: The impact of progenitor cells in atherosclerosis. *Nat Clin Pract Cardiovasc Med*, 3:94-101, 2006.
 10. Dardik A, Chen L, Frattini J, Asada H, Aziz F, Kudo FA, Sumpio BE: Differential effects of orbital and laminar shear stress on endothelial cells. *J Vasc Surg*, 41:869-880, 2005.
 11. Durand E, Scoazec A, Lafont A, Boddaert J, Al Hajzen A, Addad F, Mirshahi M, Desnos M, Tedgui A, Mallat Z: In vivo induction of endothelial apoptosis leads to vessel thrombosis and endothelial denudation: a clue to the understanding of the mechanisms of thrombotic plaque erosion. *Circulation*, 109:2503-2506, 2004.
 12. Zhou J, Lhotak S, Hilditch BA, Austin RC: Activation of the unfolded protein response occurs at all stages of atherosclerotic lesion development in apolipoprotein E-deficient mice. *Circulation*, 111:1814-1821, 2005.
 13. Gurusamy N, Das DK: Is autophagy a double-edged sword for the heart? *Acta Physiol Hung*, 96:267-276, 2009.

14. Senft D, Ronai ZA: UPR, autophagy, and mitochondria crosstalk underlies the ER stress response. *Trends Biochem Sci*, 40:141-148, 2015.
15. Kurita-Ochiai T, Jia R, Cai Y, Yamaguchi Y, Yamamoto M. Periodontal disease-induced atherosclerosis and oxidative stress. *Antioxidants*, 4: 577-590, 2015.
16. Stocker R, Keaney Jr. JF. Role of oxidative modifications in atherosclerosis. *Physiol Rev*, 84: 1381-1478, 2004.
17. Craige SM, Kant S, Reif M, Chen K, Pei Y, Angoff R, Sugamura K, Fitzgibbons T, Keaney JF: Endothelial NADPH oxidase 4 protects ApoE^{-/-} mice from atherosclerotic lesions. *Free Radic Biol Med*, 89: 1-7, 2015.
18. Vendrov AV, Hakim ZS, Madamanchi NR, Rojas M, Madamanchi C, Runge MS: Atherosclerosis is attenuated by limiting superoxide generation in both macrophage and vessel wall cells. *Arterioscler Thromb Vasc Biol*, 27: 2714-2721, 2007.
19. Cejkova S, Kralova-Lesna I, Poledne R: Monocyte adhesion to the endothelium is an initial stage of atherosclerosis development. *Cor et Vasa*, 58: e419-e425, 2016.
20. Seo JW, Yang EJ, Yoo KH, Choi IH: Macrophage differentiation from monocyte is influenced by the lipid oxidation degree of low density lipoprotein. *Mediators Inflammation*, 2015, 235797. Doi:

- 10.1155/2015/235797, 2015.
21. Tavakoli S, Asmis R: Reactive oxygen species and thiol redox signaling in the macrophage biology of atherosclerosis. *Antioxid Redox Signal*, 17: 1785-1795, 2012.
 22. Cominacini L, Pasini AF, Garbin U, Davoli A, Tosetti ML, Campagnola M, Rigoni A, Pastorino AM, Lo Cascio V, Sawamura T: Oxidized low density lipoprotein (ox-LDL) binding to ox-LDL receptor-1 in endothelial cells induces the activation of NF-kappaB through an increased production of intracellular reactive oxygen species. *J Biol Chem*, 275: 12633-12638, 2000.
 23. Creagh EM, Conroy H, Martin SJ: Caspase-activation pathways in apoptosis and immunity. *Immunol Rev*, 193:10-21, 2003.
 24. Bergsbaken T, Fink SL, Cookson BT: Pyroptosis: host cell death and inflammation. *Nat Rev Microbiol*, 7:99-109, 2009.
 25. Paglin S, Hollister T, Delohery T, Hackett N, McMahon M, Sphicas E, Domingo D, Yahalom J: A novel response of cancer cells to radiation involves autophagy and formation of acidic vesicles. *Cancer Res*, 61:439-444, 2001.
 26. Kinane JA, Benakanakere MR, Zhao J, Hosur KB, Kinane DF: *Porphyromonas gingivalis* influences actin degradation within epithelial cells during invasion and apoptosis. *Cell Microbiol*, 14:1085-1096, 2012.

27. Gargalovic PS, Gharavi NM, Clark MJ, Pagnon J, Yang WP, He A, Truong A, Baruch-Oren T, Berliner JA, Kirchgessner TG *et al*: The unfolded protein response is an important regulator of inflammatory genes in endothelial cells. *Arterioscler Thromb Vasc Biol*, 26:2490-2496, 2006.
28. Gao J, Ishigaki Y, Yamada T, Kondo K, Yamaguchi S, Imai J, Uno K, Hasegawa Y, Sawada S, Ishihara H *et al*: Involvement of endoplasmic stress protein C/EBP homologous protein in arteriosclerosis acceleration with augmented biological stress responses. *Circulation*, 124:830-839, 2011.
29. Yokouchi M, Hiramatsu N, Hayakawa K, Okamura M, Du S, Kasai A, Takano Y, Shitamura A, Shimada T, Yao J *et al*: Involvement of selective reactive oxygen species upstream of proapoptotic branches of unfolded protein response. *J Biol Chem*, 283:4252-4260, 2008.
30. Tagawa Y, Hiramatsu N, Kasai A, Hayakawa K, Okamura M, Yao J, Kitamura M: Induction of apoptosis by cigarette smoke via ROS-dependent endoplasmic reticulum stress and CCAAT/enhancer-binding protein-homologous protein (CHOP). *Free Radic Biol Med*, 45:50-59, 2008.
31. Alhusaini S, McGee K, Schisano B, Harte A, McTernan P, Kumar S, Tripathi G: Lipopolysaccharide, high glucose and saturated fatty acids induce endoplasmic reticulum stress in cultured primary human

- adipocytes: Salicylate alleviates this stress. *Biochem Biophys Res Commun*, 397:472-478, 2010.
32. Domon H, Takahashi N, Honda T, Nakajima T, Tabeta K, Abiko Y, Yamazaki K: Up-regulation of the endoplasmic reticulum stress-response in periodontal disease. *Clin Chim Acta*, 401:134-140, 2009.
33. Ogata M, Hino S, Saito A, Morikawa K, Kondo S, Kanemoto S, Murakami T, Taniguchi M, Tanii I, Yoshinaga K *et al*: Autophagy is activated for cell survival after endoplasmic reticulum stress. *Mol Cell Biol*, 26:9220-9231, 2006.
34. Shintani T, Klionsky DJ: Autophagy in health and disease: a double-edged sword. *Science*, 306:990-995, 2004.
35. Kabeya Y, Mizushima N, Ueno T, Yamamoto A, Kirisako T, Noda T, Kominami E, Ohsumi Y, Yoshimori T: LC3, a mammalian homologue of yeast Apg8p, is localized in autophagosome membranes after processing. *EMBO J*, 19:5720-5728, 2000.
36. Zhang T, Kurita-Ochiai T, Hashizume T, Oguchi S, Abiko Y, Yamamoto M: *Aggegatibacter actinomycetemcomitans* leads to endothelial apoptosis and atherosclerosis development in spontaneously hyperlipidemic mice. *Int J Oral-Med Sci*, 8: 132-141, 2010.
37. Konior A, Schramm A, Czesnikiewicz-Guzik M, Guzik TJ: NADPH oxidases in vascular pathology. *Antioxid Redox Signal*, 20: 2794-2814,

- 2014.
38. Akki A, Zhang M, Murdoch C, Brewer A, Shah AM: NADPH oxidase signaling and cardiac myocyte function. *J Mol Cell Cardiol*, 47: 15-22, 2009.
 39. Schulz E, Munzel T: NOX5, a new “radical” player in human atherosclerosis? *J Am Coll Cardiol*, 52: 1810-1812, 2008.
 40. Redza-Dutordoir M, Averill-Bates DA. Activation of apoptosis signaling pathways by reactive oxygen species. *Biochim Biophys Acta*, 1863: 2977-2992, 2016.
 41. Gambim MH, Carmo AO, Marti L, Verissimo-Filho S, Lopes LR, Janiszewski M. Platelet-derived exosomes induce endothelial cell apoptosis through peroxynitrite generation: experimental evidence for a novel mechanism of septic vascular dysfunction. *Critical Care*, 11:R107 (doi: 10. 1186/cc6133) 2007.
 42. Tricot O, Mallat Z, Heymes C, Belmin J, Leseche G, Tedgui A: Relation between endothelial cell apoptosis and blood flow direction in human atherosclerotic plaques. *Circulation*, 101: 2450-2453, 2000.
 43. Kobayashi N, DeLano FA, Schmid-Schonbein GW: Oxidative stress promotes endothelial cell apoptosis and loss of microvessels in the spontaneously hypertensive rats. *Arterioscler Thromb Vasc Biol*, 25: 2114-2121, 2005.
 44. Walford GA, Moussignac RL, Scribner AW, Loscalzo J, Leopold JA:

Hypoxia potentiates nitric oxide-mediated apoptosis in endothelial cells via peroxynitrite-induced activation of mitochondria-dependent and -independent pathways. *J Biol Chem*, 279: 4425-4432, 2004.

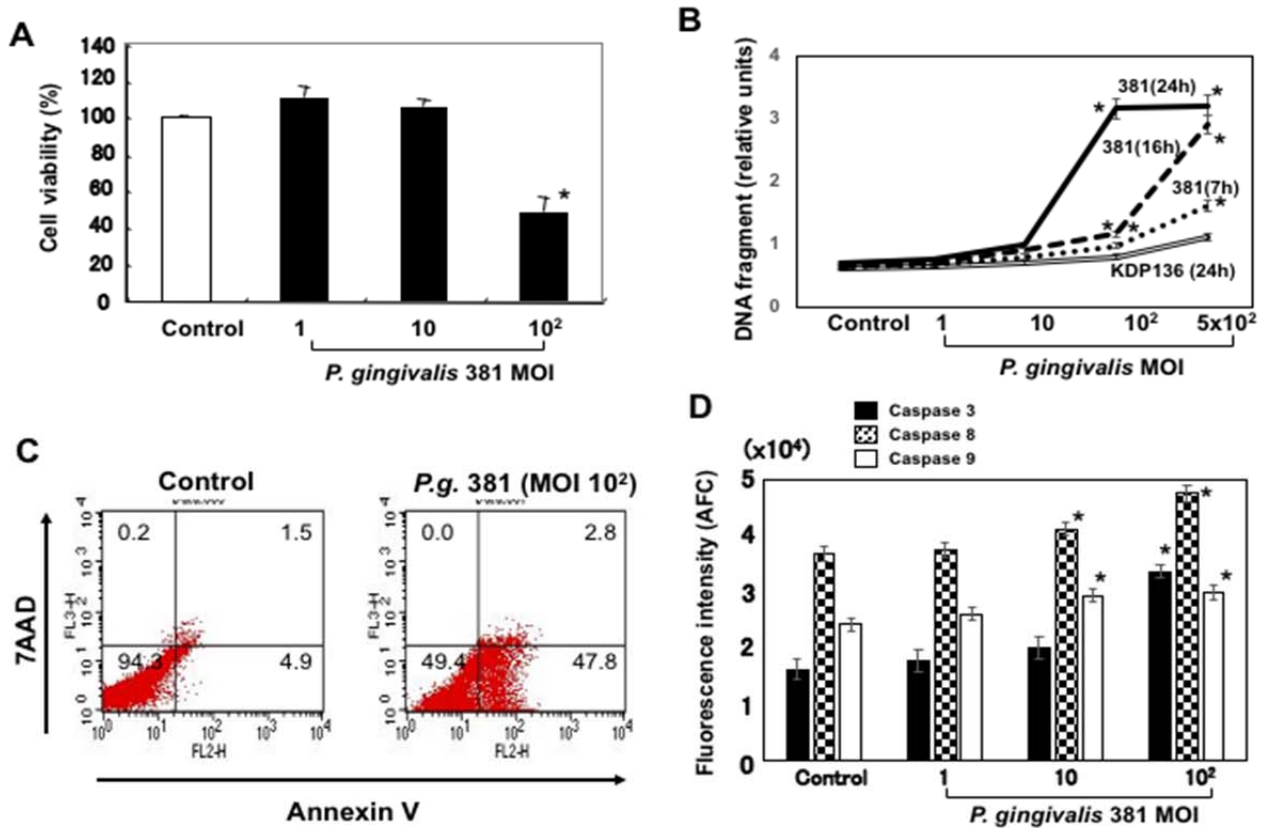


Fig. 1. *P. gingivalis* infection inhibits cellular viability and induces apoptosis in HUVEC. (A) HUVEC were treated with *P. gingivalis* 381 at an MOI of 1:1- 1:10² for 21 h. Cell viability was determined using a Cell Counting Kit-8 (CCK-8). The data are expressed as the mean \pm SEM of 3 different experiments. * $p < 0.05$ vs bacteria-free control cells. (B) HUVEC were treated with *P. gingivalis* 381 at an MOI of 1:1- 1:5 \times 10² for 7, 16, and 24 h, and with KDP136 at an MOI of 1:1- 1:5 \times 10² for 24 h. Cellular apoptosis was quantified by DNA fragmentation using the Cell Death Detection ELISA^{PLUS} Kit as described in materials and methods. Data are expressed as the mean \pm SEM of 3 different experiments. * $p < 0.05$ vs bacteria-free control

cells. (C) HUVEC were stained with annexin V-EnzoGold and 7-AAD after treatment with *P. gingivalis* 381 at an MOI of 1:10² for 21 h and then they were analyzed by flow cytometry. The figure is representative of three experiments with similar results. (D) HUVEC were treated with *P. gingivalis* 381 at an MOI of 1:1 - 1:10² for 16 h. Cell extracts were prepared and caspase activities were measured. Data are expressed as the mean ± SEM of 3 different experiments. **p* < 0.05 vs bacteria-free control cells.

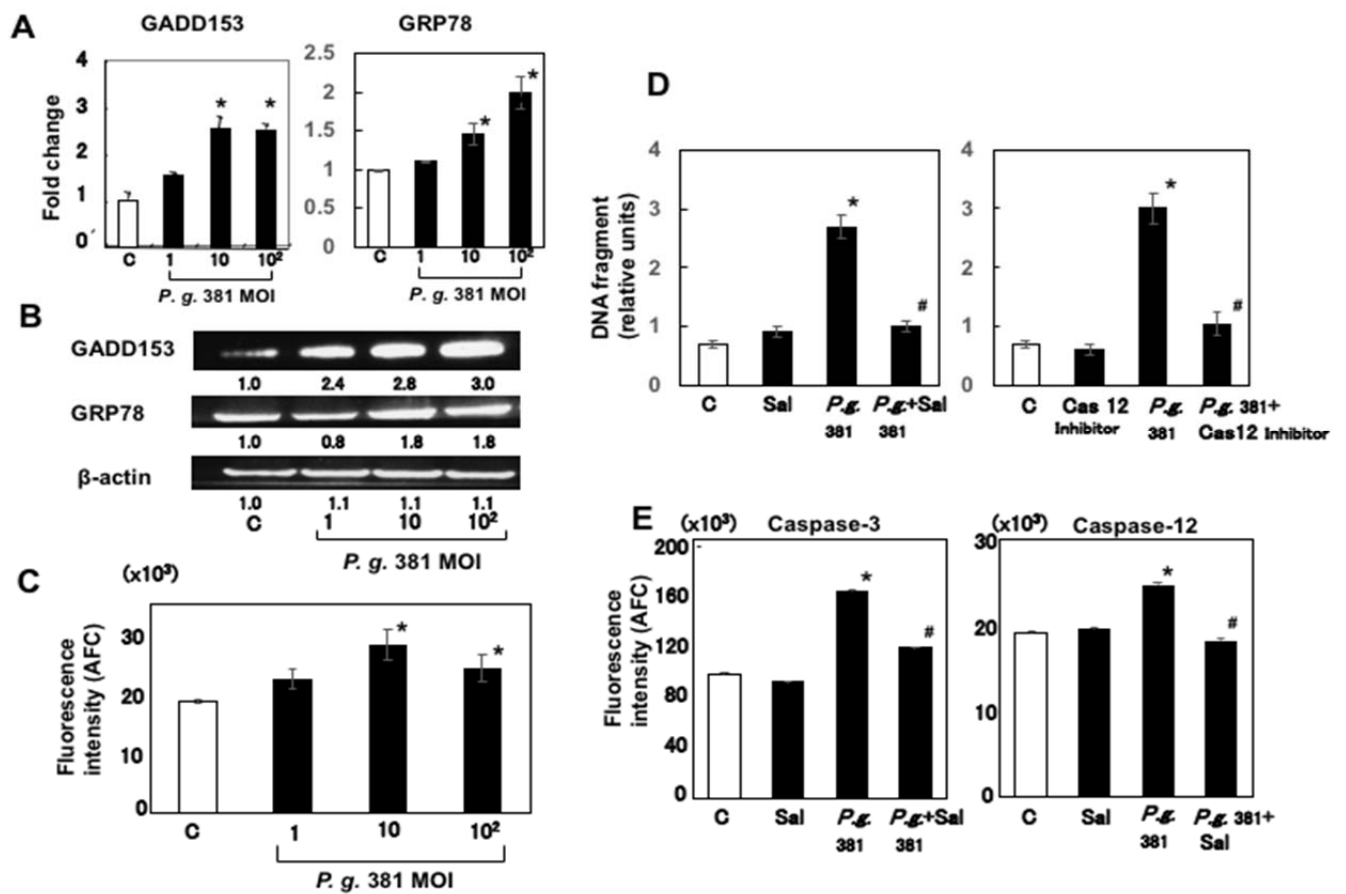


Fig. 2. *P. gingivalis* 381 induces UPR like response in HUVEC. (A) HUVEC were treated with *P. gingivalis* 381 at an MOI of 1:1 - 1:10² for 8 h. Quantitative real-time PCR analysis was performed for GADD153 and GRP78 relative to β -actin expression. Data are expressed as the mean \pm SEM of 3 different experiments. * p < 0.01 vs bacteria-free control cells. (B) HUVEC were treated with *P. gingivalis* 381 at an MOI of 1:1 - 1:10² for 21 h. Whole cell lysates were subjected to SDS-PAGE, followed by Western blot analysis using antibodies to GADD153 and GRP78. Levels of β -actin were also detected as an internal control. The density of each band was measured

by densitometry, and the relative band densities were calculated by comparing the band densities with those of the control. (C) HUVEC were treated with *P. gingivalis* 381 at an MOI of 1:1 - 1:10² for 16 h. Cell extracts were then prepared and caspase-12 activity measured. Data are expressed as the mean ± SEM of 3 different experiments. **p* < 0.01 vs bacteria-free control cells. (D) HUVEC were pre-treated with a caspase-12 or ER stress inhibitor for 1 h and then treated with *P. gingivalis* 381 at an MOI of 1:10² for 24 h. The ratio of apoptotic cells to total cells was determined using the Cell Death Detection ELISA^{PLUS} Kit. Data are expressed as the mean ± SEM of 3 different experiments. **p* < 0.01 vs bacteria-free control cells. #*p* < 0.01 vs bacteria-treated control cells. (E) HUVEC were pre-treated with an ER stress inhibitor for 1 h and then treated with *P. gingivalis* 381 at an MOI of 1:10² for 16 h. Cell extracts were then prepared and caspase activity measured. Data are expressed as the mean ± SEM of 3 different experiments. **p* < 0.01 vs bacteria-free control cells. #*p* < 0.01 vs bacteria-treated control cells.

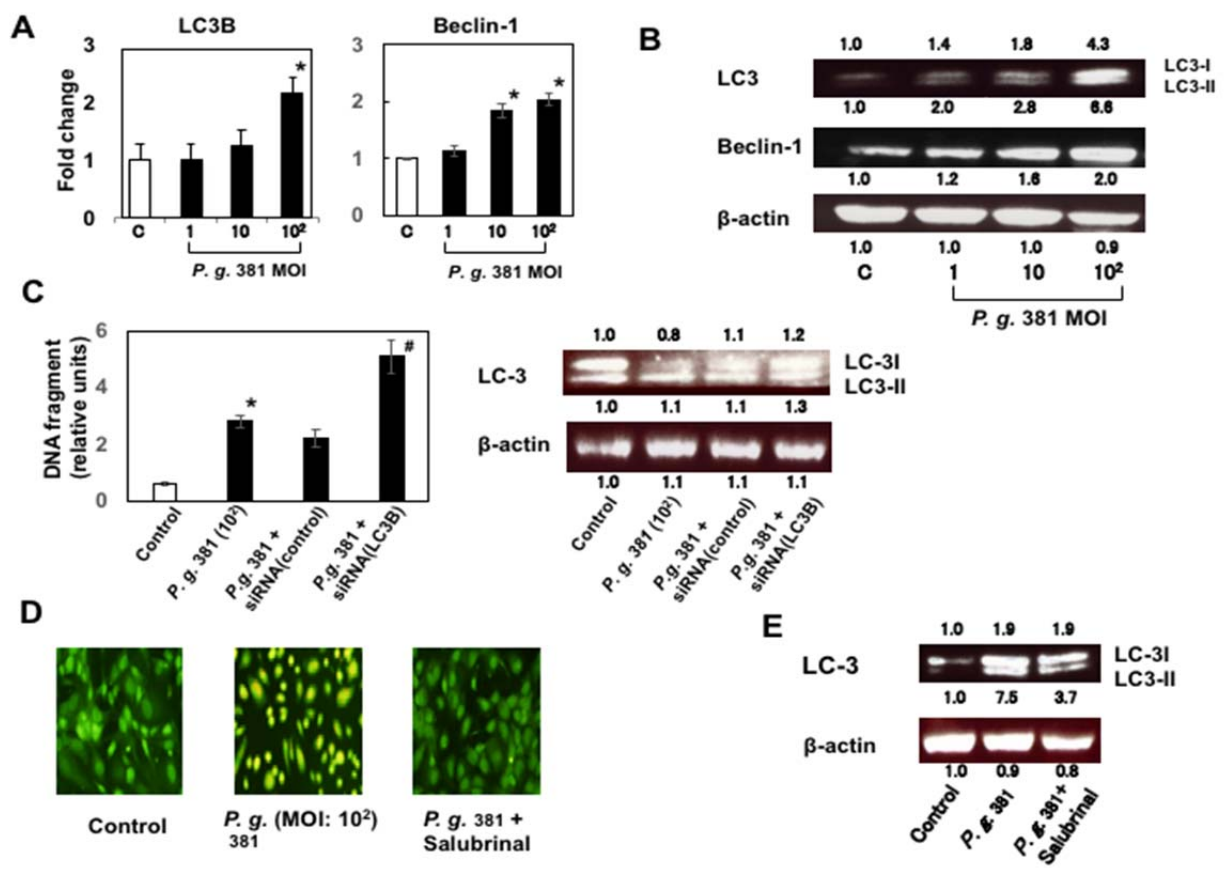


Fig. 3. *P. gingivalis* 381 triggers ER stress-induced autophagy in HUVEC. (A) HUVEC were treated with *P. gingivalis* 381 at an MOI of 1:1 - 1:10² for 8 h. Quantitative real-time PCR analysis was performed for LC3B and Beclin-1 relative to β -actin expression. Data are expressed as the mean \pm SEM of 3 different experiments. * p < 0.01 vs bacteria-free control cells.

(B) HUVEC were treated with *P. gingivalis* 381 at an MOI of 1:1 - 1:10² for 21 h. Whole cell lysates were subjected to SDS-PAGE, followed by Western blot analysis using antibodies to LC3 and Beclin-1. Levels of β -actin were also detected as an internal control. The density of each band was measured by densitometry, and the relative band densities were calculated by comparing

the band densities with those of the control. (C) HUVEC were transfected with 50 nM of LC3B specific siRNA or control siRNA and then stimulated with *P. gingivalis* 381 at an MOI of 1:10² for 24 h (DNA fragment) or 16 h (Western blotting). The ratio of apoptotic cells to total cells was determined using the Cell Death Detection ELISA^{PLUS} Kit. Data are expressed as the mean ± SEM of 3 different experiments. **p* < 0.01 vs bacteria-free control cells. #*p* < 0.01 vs non-transfected or control siRNA-treated cells. The expression of LC3 was analyzed by western blotting. Lysates were then immunoblotted with anti-LC-3. Levels of β-actin were also detected as an internal control. (D) HUVEC were pre-treated with an ER stress inhibitor for 1 h and then treated with *P. gingivalis* 381 at an MOI of 1:10² for 8 h. Acridine orange staining indicated that the ER stress inhibitor suppressed autophagic vacuolation induced by *P. gingivalis* 381. (E) HUVEC were pre-treated with an ER stress inhibitor for 1 h and then treated with *P. gingivalis* 381 at an MOI of 1:10² for 21 h. Whole cell lysates were subjected to SDS-PAGE, followed by Western blot analysis using antibodies to LC3. Levels of β-actin were also detected as an internal control. The density of each band was measured by densitometry, and the relative band densities were calculated by comparing the band densities with those of the control.

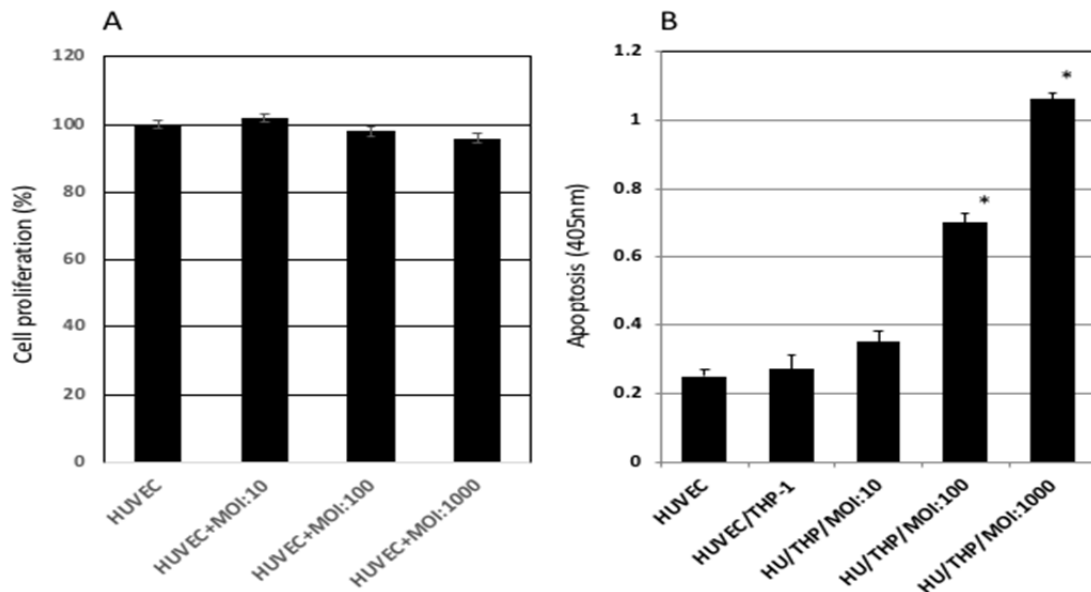


Fig. 4. *Aa* induces HUVEC apoptosis in HUVEC/monocyte co-culture system.

(A) HUVEC were treated with *Aa* at an MOI of 1:10 - 1:1000 for 21 h. Cell viability was determined using a BrdU cell proliferation ELISA kit. The data are expressed as the mean \pm SEM of 3 different experiments. (B) HUVEC was indirectly cocultured with THP-1 cells and *Aa* at an MOI of 1:10 - 1:1000 for 16 h using 0.4 μ M pore size cell culture inserts. Cellular apoptosis was quantified by DNA fragmentation using the Cell Death Detection ELISA^{PLUS} Kit as described in materials and methods. Data are expressed as the mean \pm SEM of 3 different experiments. * $p < 0.05$ vs bacteria-free control cells.

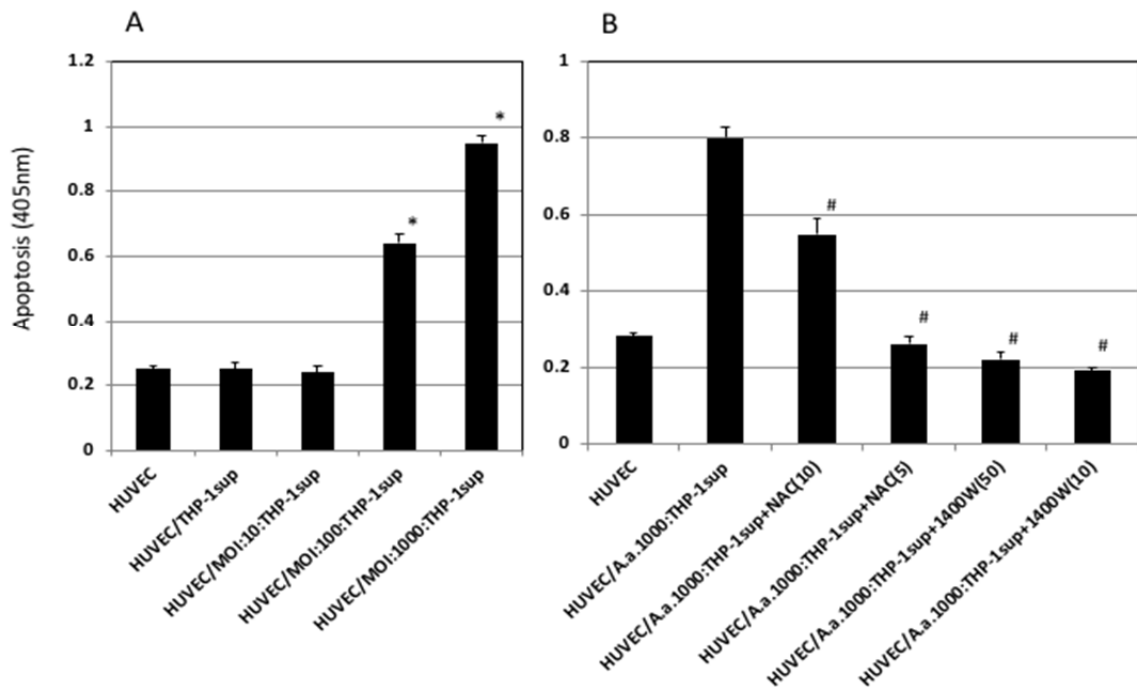


Fig. 5. *Aa*-sensitized monocyte culture supernatant induces HUVEC apoptosis. (A) HUVEC was co-cultured for 16 h with tenths volume of culture supernatant of THP-1 cells which previously sensitized with *Aa* at an MOI of 1:10 - 1:1000 for 16 h. Cellular apoptosis was quantified by DNA fragmentation using the Cell Death Detection ELISA^{PLUS} Kit as described in materials and methods. Data are expressed as the mean \pm SEM of 3 different experiments. * $p < 0.05$ vs bacteria-free control cells. (B) HUVEC was co-cultured for 16 h with tenths volume of culture supernatant of THP-1 cells which previously sensitized with *Aa* at an MOI of 1:1000 for 16 h. For the apoptosis inhibition assays, THP-1 cells were preincubated for 1h with the

NAC (5 or 10 mM) or 1400W (10 or 50 μ M) before sensitization with *Aa*.

Cellular apoptosis was quantified Data are expressed as the mean \pm SEM of 3 different experiments. * $p < 0.05$ vs bacteria-free control cells. # $p < 0.05$ vs *Aa* sensitized cells.

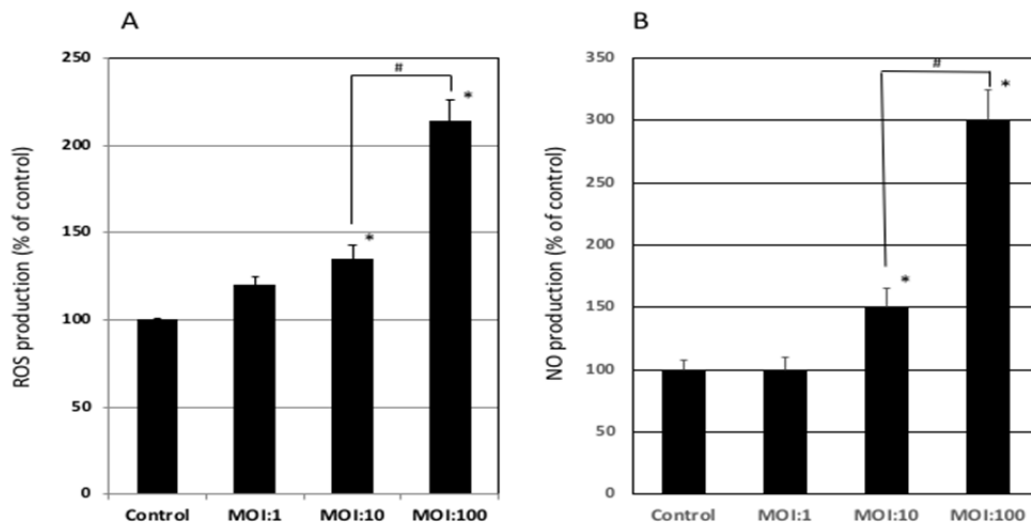


Fig. 6. *Aa* induces ROS and NO Production in monocytes. *Aa* was added to nearly confluent THP-1 cells at an MOI of 1:1 - 1:100 and incubated at 37°C for 30 min. (A) The formation of a fluorescent product, dichlorofluorescein, was analyzed using a fluorescence spectrometer. (B) Total nitrite was measured using Bioxytech nitric oxide assay kit. Data are expressed as the mean \pm SEM of 3 different experiments. * $p < 0.01$ vs bacteria-free control cells. # $p < 0.01$ vs *Aa* (MOI:10)-sensitized cells.

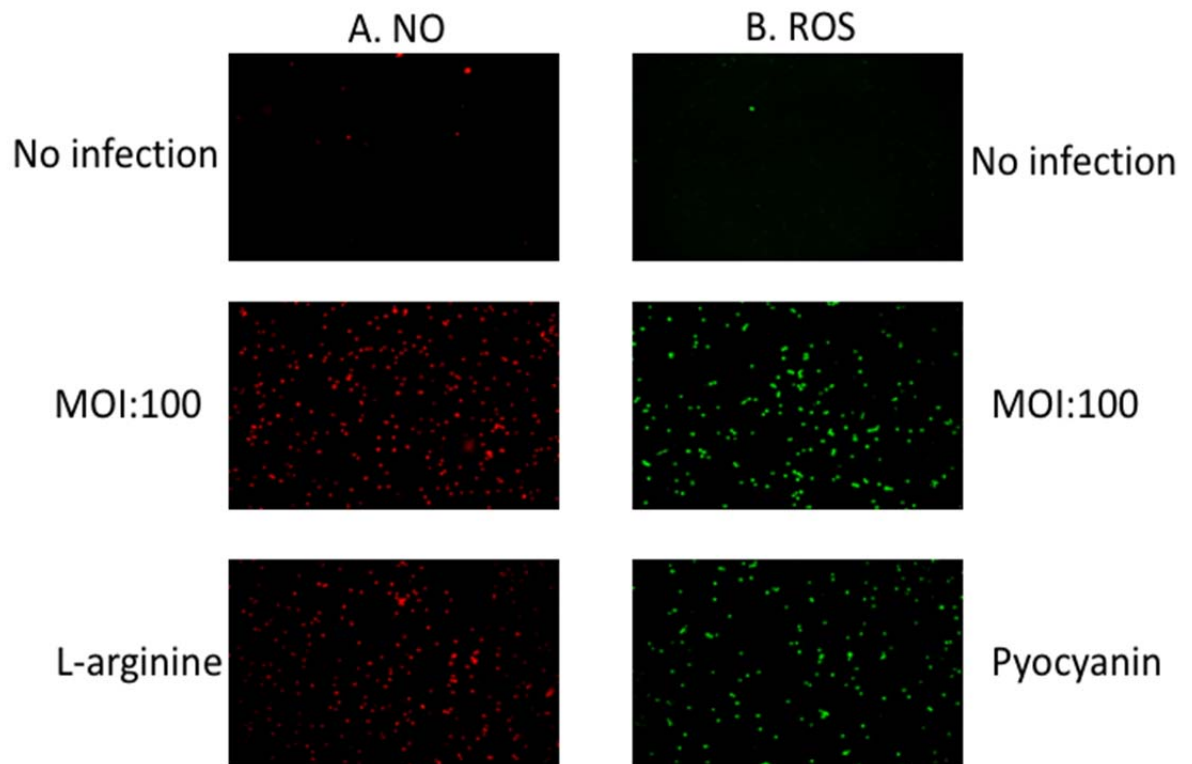


Fig. 7. NO and ROS detection in *Aa*-sensitized monocytes. THP-1 cells were treated with *Aa* at an MOI of 1:1 - 1:100 for 30 min and analyzed under fluorescence microscope.

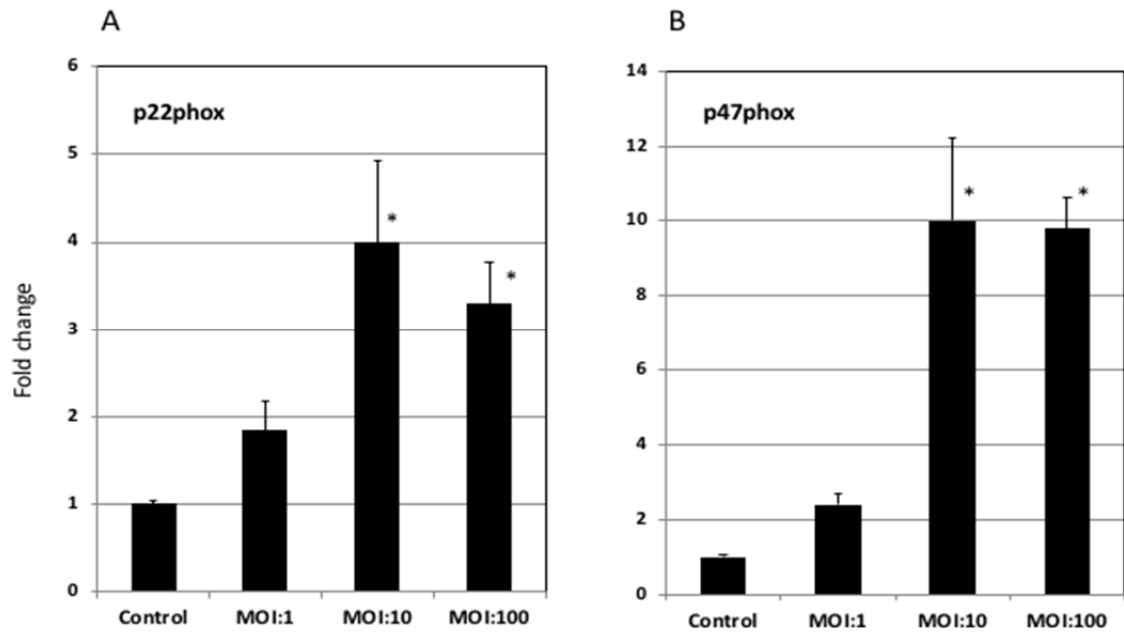


Fig. 8. *Aa* increases gene expression of p22phox and p47phox in monocytes.

THP-1 cells were treated with *Aa* at an MOI of 1:1 - 1:100 for 8 h.

Quantitative real-time PCR analysis was performed for p22phox and p47phox relative to GAPDH expression. Data are expressed as the mean \pm SEM of 3 different experiments. * $p < 0.01$ vs bacteria-free control cells.

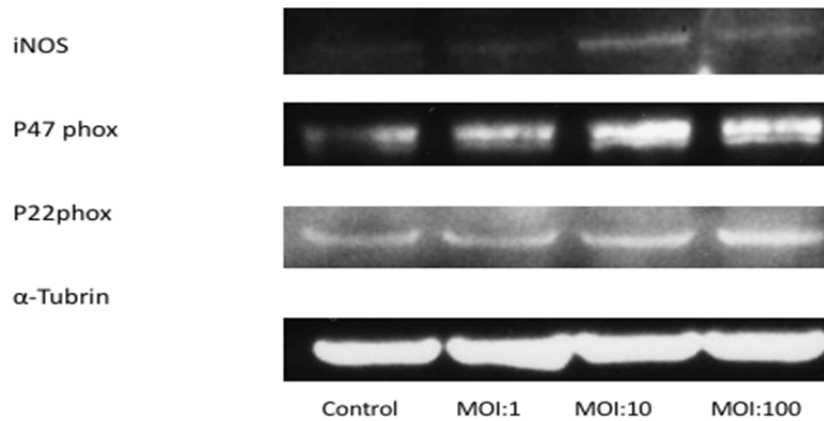


Fig. 9. *Aa* increases protein expression of iNOS, p22phox and p47phox in monocytes. THP-1 cells were treated with *Aa* at an MOI of 1:1 - 1:100 for 16 h. Whole cell lysates were subjected to SDS-PAGE, followed by Western blot analysis using antibodies to iNOS, p22phox and p47phox. Levels of α -Tubrin were also detected as an internal control.

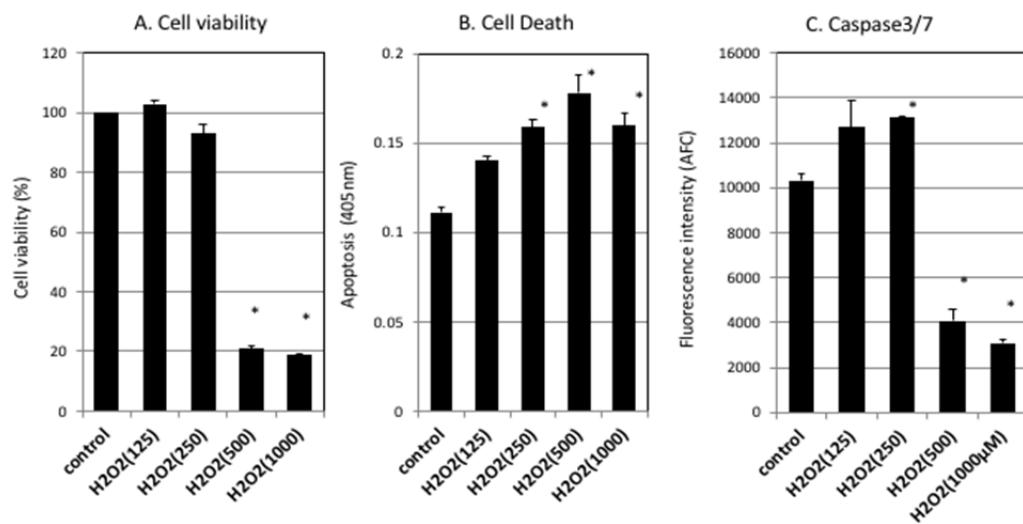


Fig. 10. ROS such as H₂O₂ induce apoptosis. (A) HUVEC treated with H₂O₂ (125-1000 μM) for 21 h to determine cell viability. (B) HUVEC treated with H₂O₂ (125-1000 μM) for 16 h to quantify cellular apoptosis. (C) HUVEC treated with H₂O₂ (125-1000 μM) for 8 h to measure caspase activities. Data are expressed as the mean ± SEM of 3 different experiments. **p* < 0.05 vs H₂O₂-free control cells.